

Vapor–Liquid Equilibria of Water + Alkylimidazolium-Based Ionic Liquids: Measurements and Perturbed-Chain Statistical Associating Fluid Theory Modeling

Helena Passos,^{†,⊥} Imran Khan,^{†,⊥} Fabrice Mutelet,[‡] Mariana B. Oliveira,[†] Pedro J. Carvalho,[†] Luís M. N. B. F. Santos,[§] Christoph Held,^{*,||} Gabriele Sadowski,^{||} Mara G. Freire,[†] and João A. P. Coutinho^{*,†}

[†]Departamento de Química, CICECO, Universidade de Aveiro, Campus Universitário de Santiago, 3810-193 Aveiro, Portugal

[‡]Université de Lorraine, Ecole Nationale Supérieure des Industries Chimiques, Laboratoire Réactions et Génie des Procédés, CNRS (UMR7274), 1 rue Grandville, BP 20451 54001 Nancy, France

[§]Centro de Investigação em Química, Departamento de Química e Bioquímica, Faculdade de Ciências, Universidade do Porto, Rua do Campo Alegre, 687, 4169-007 Porto, Portugal

^{||}Laboratory of Thermodynamics, Department of Biochemical and Chemical Engineering, Technische Universität Dortmund, Emil-Figge-Str. 70, 44227 Dortmund, Germany

S Supporting Information

ABSTRACT: The industrial application of ionic liquids (ILs) requires the knowledge of their physical properties and phase behavior. This work addresses the experimental determination of the vapor–liquid equilibria (VLE) of binary systems composed of water + imidazolium-based ILs. The ILs under consideration are 1-butyl-3-methylimidazolium trifluoromethanesulfonate, 1-butyl-3-methylimidazolium thiocyanate, 1-butyl-3-methylimidazolium tosylate, 1-butyl-3-methylimidazolium trifluoroacetate, 1-butyl-3-methylimidazolium bromide, 1-butyl-3-methylimidazolium chloride, 1-butyl-3-methylimidazolium methanesulfonate, and 1-butyl-3-methylimidazolium acetate, which allows the evaluation of the influence of the IL anion through the phase behavior. Isobaric VLE data were measured at 0.05, 0.07, and 0.1 MPa for IL mole fractions ranging between 0 and 0.7. The observed increase in the boiling temperatures of the mixtures is related with the strength of the interaction between the IL anion and water. The Perturbed-Chain Statistical Associating Fluid Theory (PC-SAFT) was further used to describe the obtained experimental data. The ILs were treated as molecular associating species with two association sites per IL. The model parameters for the pure fluids and the binary interaction parameter k_{ij} between water and ILs were determined by a simultaneous fitting to pure-IL densities, water activity coefficients at 298.15 K and VLE data at 0.1 MPa. Pure-IL densities, water activity coefficients, and VLE data were well described by PC-SAFT in broad temperature, pressure, and composition ranges. The PC-SAFT parameters were applied to predict the water activity coefficients at infinite dilution in ILs, and a satisfactory prediction of experimental data was observed.

■ INTRODUCTION

The absorption refrigeration is widely used in many fields, such as in military, air conditioning, electric power, steelmaking, chemical industry, and drugs manufacturing.¹ This technology requires a working pair of fluids composed of refrigerant and absorbent. Many working fluid pairs are suggested in literature^{2–5} for absorption refrigeration, but there is still no ideal working fluid pair by now. The performance of absorption cycles depends on the thermodynamic properties of the working pair. Currently, the binary systems water + NH₃ and water + LiBr are applied as working fluid pairs in absorption refrigerators,² but these systems have some disadvantages such as corrosion, crystallization, or toxicity. Therefore, the finding of more advantageous working pairs with good thermal stability without corrosive and crystallization effects has become a research focus in recent years. Several researchers^{3–5} demonstrated that the extreme values of the excess Gibbs function (G_{\max}^E) can be used to evaluate the performance of the absorption cycle working pairs. Mixtures with negative

deviation from the Raoult's law usually exhibit a strong absorption performance. The G_{\max}^E of such mixtures are negative as the activity coefficients of the respective components are lower than unity. This causes large vapor pressure depressions and/or high boiling-point elevations.

Ionic liquids (ILs) have recently attracted increased attention because of their potential for absorption refrigeration.⁶ Due to their physical properties, ILs can be used as new cooling absorbents for absorption chillers or absorption heat pumps where one possible working pair might be composed of water (refrigerant) and IL (absorber). Thus, knowledge about thermodynamic properties and phase equilibria of water + IL solutions is fundamental to determine their applicability as

Received: December 5, 2013

Revised: February 5, 2014

Accepted: February 10, 2014

Published: February 10, 2014

absorption refrigeration systems^{7,8} and for a correct design and application of absorption processes.

A good working fluid pair for absorption refrigeration processes should show a large boiling-temperature elevation and/or vapor pressure depression. The boiling-temperature elevation of water depends on the kind of IL, on the IL concentration in the mixture and on temperature. For absorption systems using water + ILs, numerous literature works have been reported.^{8–12} Experimental activity coefficients of water at infinite dilution in ILs, γ_w^∞ , have also been extensively published.^{13–34} Such data are an appropriate indicator for the evaluation of the performance of a working pair for absorption refrigeration processes. For this application, low γ_w^∞ values are desired, meaning strong water–IL interactions.

Yokozeki and Shiflett stated that an optimized water + IL system could compete with the existing water + LiBr system³⁵ for absorption refrigeration processes. Zuo et al.⁸ suggested the system water + 1-ethyl-3-methylimidazolium ethylsulfate ($[\text{C}_2\text{C}_1\text{im}][\text{C}_2\text{H}_5\text{SO}_4]$) as a new working pair. Wang et al.³⁶ proposed the application of the system constituted by water + 1,3-dimethylimidazolium chloride ($[\text{C}_1\text{C}_1\text{im}]\text{Cl}$) as an alternative working pair for absorption cycles based on the measurement of the binary vapor–liquid equilibrium (VLE) data. Kim et al.³⁷ showed broad theoretical work on various mixtures of refrigerants and ILs as working pairs for the absorption refrigeration system, and Zhang et al.⁹ simulated a single-effect absorption cycle using the water + 1,3-dimethylimidazolium dimethylphosphate ($[\text{C}_1\text{C}_1\text{im}][\text{DMP}]$) and water + 1-ethyl-3-methylimidazolium dimethylphosphate ($[\text{C}_2\text{C}_1\text{im}][\text{DMP}]$) systems. Wu et al.³⁸ measured vapor pressures and the VLE of water + 1,3-dimethylimidazolium tetrafluoroborate ($[\text{C}_1\text{C}_1\text{im}][\text{BF}_4]$) mixtures and suggested them as promising working pairs on a comparison basis with $[\text{C}_1\text{C}_1\text{im}]\text{Cl}$ ³⁸ and 1-butyl-3-methylimidazolium tetrafluoroborate ($[\text{C}_4\text{C}_1\text{im}][\text{BF}_4]$).³⁹ Kim et al.³⁹ measured the vapor pressures of water + 1-butyl-3-methylimidazolium bromide ($[\text{C}_4\text{C}_1\text{im}]\text{Br}$), water + $[\text{C}_4\text{C}_1\text{im}][\text{BF}_4]$ and water + 1-(2-hydroxyethyl)-3-methylimidazolium tetrafluoroborate ($[\text{OHC}_2\text{C}_1\text{im}][\text{BF}_4]$) systems in broad concentration and temperature ranges. Nie et al.¹⁰ suggested water + 1-(2-hydroxyethyl)-3-methylimidazolium chloride ($[\text{OHC}_2\text{C}_1\text{im}]\text{Cl}$) as a novel alternative working pair for the absorption heat pump cycle. The vapor pressure and specific heat capacity of binary solutions of 1-ethyl-3-ethylimidazolium diethylphosphate ($[\text{C}_2\text{C}_2\text{im}][\text{DEP}]$),⁴⁰ $[\text{C}_1\text{C}_1\text{im}][\text{DMP}]$,⁴¹ $[\text{C}_2\text{C}_1\text{im}][\text{DMP}]$,⁴² and 1-butyl-3-methylimidazolium dibutylphosphate ($[\text{C}_4\text{C}_1\text{im}][\text{DBP}]$)⁴¹ with water, ethanol, or methanol were also investigated as new working pairs. Recently, Carvalho et al.⁴³ measured the VLE of 1-ethyl-3-methylimidazolium chloride ($[\text{C}_2\text{C}_1\text{im}]\text{Cl}$), 1-butyl-3-methylimidazolium chloride ($[\text{C}_4\text{C}_1\text{im}]\text{Cl}$), 1-hexyl-3-methylimidazolium chloride ($[\text{C}_6\text{C}_1\text{im}]\text{Cl}$), and choline chloride ($[\text{N}_{111}(\text{2OH})]\text{Cl}$) with water and ethanol using a new isobaric microbulliometer at pressures ranging from 0.05 to 0.1 MPa. These binary systems present negative deviations from Raoult's Law and negative excess enthalpies, suggesting that some of them could be appropriate working pairs for absorption chillers or absorption heat pumps.

Several thermodynamic models have been applied to describe thermodynamic properties and phase equilibria of IL aqueous solutions, namely activity-coefficient models, equations of state (EoS), and unimolecular quantum chemistry calculations. For instance, Domańska and Marciniak described

the liquid–liquid equilibrium (LLE) and the solid–liquid equilibrium (SLE) of the 1-butyl-3-methylimidazolium bis-(trifluoromethylsulfonyl)amide ($[\text{C}_4\text{C}_1\text{im}][\text{NTf}_2]$) aqueous system with the Non-Random Two-Liquid (NRTL) and the Wilson models.⁴⁴ The VLE of the same system was also described with the modified UNiversal Functional Activity Coefficients (UNIFAC) by Nebig et al.⁴⁵ Li et al.⁴⁶ applied the Square-Well Chain Fluid with Variable Range EoS (SWCF-VR) to model thermodynamic properties of aqueous solutions of ILs, and Wang et al.⁴⁷ used the same EoS to describe the VLE of several systems constituted by water + $[\text{NTf}_2]$ -based ILs. Banarjee et al.⁴⁸ applied the CONductor-like Screening MODEL for Realistic Solvation (COSMO-RS)—a predictive model based on unimolecular quantum chemistry calculations—to predict the VLE of water + alkylimidazolium-based ILs. Freire et al.^{49–51} also studied the VLE and LLE of a large range of water + IL mixtures using COSMO-RS. Carvalho et al.⁴³ recently applied the NRTL model to correlate VLE data of binary mixtures of water + IL and ethanol + IL and the nonideal behavior of the liquid phase solutions.

In recent years, a physically grounded theoretical approach, the Statistical Associating Fluid Theory (SAFT), has been shown to be able to describe thermophysical properties and phase behaviors of ILs as well as their mixtures. Within this framework, the strong interactions between anions and cations are represented through specific association sites. Vega et al.⁵² used soft-SAFT to describe the LLE of water + imidazolium-based ILs,⁵³ using three maximum association sites mimicking the strong interactions between the anion and the cation. Padaszyński and Domańska used the Perturbed-Chain Statistical Associating Fluid Theory (PC-SAFT) to calculate the LLE and the SLE of water + ILs. The authors modeled the ILs using ten association sites to represent the cation–anion interactions.⁵⁴ Nann et al.⁵⁵ modeled 1-butanol + IL mixtures with the 2B association approach for ILs in order to predict the LLE of water + 1-butanol + IL systems accurately with PC-SAFT. Ji et al.⁵⁶ used ePC-SAFT to predict the CO_2 solubilities in ILs with pure-IL parameters obtained from the fitting to pure-IL liquid densities.

In this work, the VLE (T, x) of several systems composed of water + imidazolium-based ILs, covering different families of anions, were experimentally measured at different pressures and in a broad composition range. In addition, the PC-SAFT EoS, using two association sites *per* molecular IL, was used to describe the experimental data. PC-SAFT parameters for the molecular ILs were regressed to pure-IL density data, VLE and water activity coefficient data of the studied mixtures. In a second step, these parameters were applied to predict the water infinite dilution activity coefficients of some water + IL systems and a comparison with literature and experimental data measured in this work is presented and discussed.

The physical properties of pure ILs and the phase behavior of water + IL mixtures strongly depend on the IL cation and anion.⁵⁷ In this work, new insights regarding IL–water interactions were inferred through the new experimental data and the respective PC-SAFT modeling.

■ EXPERIMENTAL SECTION

Materials. Eight imidazolium-based ILs were investigated, namely 1-butyl-3-methylimidazolium trifluoromethanesulfonate ($[\text{C}_4\text{C}_1\text{im}][\text{CF}_3\text{SO}_3]$), 1-butyl-3-methylimidazolium thiocyanate ($[\text{C}_4\text{C}_1\text{im}][\text{SCN}]$), 1-butyl-3-methylimidazolium tosylate ($[\text{C}_4\text{C}_1\text{im}][\text{TOS}]$), 1-butyl-3-methylimidazolium trifluoroacetate

tate ($[\text{C}_4\text{C}_1\text{im}][\text{CF}_3\text{CO}_2]$), 1-butyl-3-methylimidazolium bromide ($[\text{C}_4\text{C}_1\text{im}]\text{Br}$), 1-butyl-3-methylimidazolium chloride ($[\text{C}_4\text{C}_1\text{im}]\text{Cl}$), 1-butyl-3-methylimidazolium methanesulfonate ($[\text{C}_4\text{C}_1\text{im}][\text{C}_1\text{SO}_3]$), and 1-butyl-3-methylimidazolium acetate ($[\text{C}_4\text{C}_1\text{im}][\text{C}_1\text{CO}_2]$). The chemical structures of these ILs are shown in Figure 1. The ILs were obtained from IoLiTec

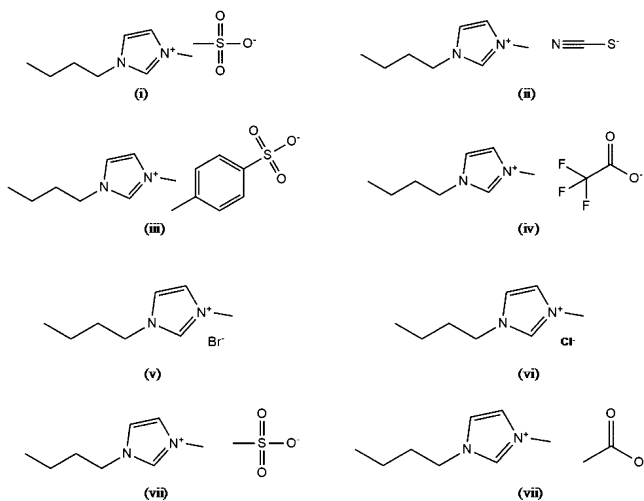


Figure 1. Chemical structures of the studied ILs (i) $[\text{C}_4\text{C}_1\text{im}][\text{CF}_3\text{SO}_3]$; (ii) $[\text{C}_4\text{C}_1\text{im}][\text{SCN}]$; (iii) $[\text{C}_4\text{C}_1\text{im}][\text{TOS}]$; (iv) $[\text{C}_4\text{C}_1\text{im}][\text{CF}_3\text{CO}_2]$; (v) $[\text{C}_4\text{C}_1\text{im}]\text{Br}$; (vi) $[\text{C}_4\text{C}_1\text{im}]\text{Cl}$; (vii) $[\text{C}_4\text{C}_1\text{im}][\text{C}_1\text{SO}_3]$; and (viii) $[\text{C}_4\text{C}_1\text{im}][\text{C}_1\text{CO}_2]$.

(Germany), with mass fraction purities higher than 98 wt %. To reduce the content of water and volatile organics to negligible values, high vacuum (10^3 Pa) and stirring at moderate temperature (303 K), for a period of at least 48 h, were applied prior to the measurements. The final water content of the ILs was determined with a Metrohm 831 Karl Fischer coulometer (Switzerland), using the Hydranal-Coulomat E from Riedel-de Haen as analyte, indicating a water mass fraction percentage lower than 30×10^{-6} wt %. The purity of each IL was further confirmed by ^1H and ^{13}C NMR using a Bruker Avance 300 spectrometer (Germany). The water used was double distilled and deionized.

Experimental Equipment. Vapor–Liquid Equilibria. The VLE studies were carried out in an isobaric microbulliometer at different fixed pressures of 0.05, 0.07, and 0.1 MPa. The isobaric microbulliometer apparatus used, and methodology is described in detail elsewhere.⁴³

The equilibrium temperature of the liquid phase was measured, with an uncertainty of 0.05 K, with a fast response glass-sealed Pt100 class 1/10, which was calibrated prior to the measurements by comparison with a NIST-certified Fluke RTD25 standard thermometer (U.S.A.). The internal pressure of the ebulliometer was kept constant through a vacuum pump Büchi V-700 and a V-850 Büchi (Switzerland), for pressure monitoring and pressure controller unit. Pressure was measured with a Baratron type capacitance Manometer, MKS model 728A (U.S.A.), with an accuracy of 0.5%. This equipment was placed in the vacuum line away from the microbulliometer. Equilibrium was assumed after 30 min of constant and smooth boiling (reflux) at constant pressure. The mixture composition was determined with an Anton Paar Abbemat 500 Refractometer (Austria), with an uncertainty of 2×10^{-5} nD, using a calibration curve established prior to the measurements. The adequacy of the apparatus to measure this type of systems was

previously confirmed.⁴³ Additionally, the apparatus was applied to measure the VLE of pure compounds (ethanol, water, *p*-xylene, and decane) covering the temperature range of interest for the water + IL systems studied in this work. An uncertainty of the boiling temperatures of 0.1 K was observed. The IL was kept under moderate vacuum (1 Pa) for at least 30 min before the measurements to ensure no water absorption from atmosphere during equilibration.

Activity Coefficients at Infinite Dilution. Inverse chromatography experiments were carried out using a Bruker 450-GC gas chromatograph equipped with a heated on-column injector and a TCD detector. The injector and detector temperatures were kept constant at 523 K during all experiments. To obtain adequate retention times, the helium flow rate was adjusted. Air was used to determine the column hold-up time. Exit gas flow rates were measured with a soap bubble flow meter. The temperature of the oven was determined with a Pt100 probe and controlled with an uncertainty of 0.1 K. A computer directly recorded the detector signals and the corresponding chromatograms were generated using the Galaxie Chromatography Software. Using a rotary evaporation preparatory technique, 1.0 m length columns were packed with a stationary phase, consisting of 0.20 to 0.35 mass fraction of IL on Chromosorb WHP (60–80 mesh) sorbent media. After the solvent (ethanol) evaporation, under vacuum, the support was left to equilibrate, at 333 K during 6 h. Prior to the measurements, each packed column was conditioned for 12 h at 363 K with a helium flow rate of $20 \text{ cm}^3 \cdot \text{min}^{-1}$. The packing level was calculated from the masses of the packed and empty columns and was checked throughout experiments. The weight of the stationary phase was determined with a precision of ± 0.0003 g. A headspace sample volume of $(1-5) \times 10^{-3} \text{ cm}^3$ was injected to satisfy infinite dilution conditions. In order to confirm reproducibility, each experiment was repeated at least thrice. Retention times were rigorously reproducible with an uncertainty of 0.5–2 s. To verify the stability under these experimental conditions, ruling out elution of the stationary phase by the helium stream, measurements of retention time were repeated systematically each day for three solutes. No changes in the retention times were observed during this study.

The retention data garnered by inverse chromatography experiments were used to calculate partition coefficients of water in the different ILs. The standardized retention volume, V_{N} , was calculated following the relationship:^{58,59}

$$V_{\text{N}} = J U_0 t'_{\text{R}} \frac{T_{\text{col}}}{T_{\text{rt}}} \left(1 - \frac{p_{\text{w}}^0}{p_{\text{out}}} \right) \quad (1)$$

where the adjusted retention time, t'_{R} , was taken as the difference between the retention time of water and that of air, T_{col} is the column temperature, U_0 is the flow rate of the carrier gas measured at room temperature (T_{rt}), p_{w}^0 is the vapor pressure of water at T_{rt} and p_{out} is the outlet pressures.

The factor J in eq 1 corrects for the influence of the pressure drop along the column and is given through the relation:^{58,59}

$$J = \frac{3}{2} \frac{\left[\left(\frac{p_{\text{in}}}{p_{\text{out}}} \right)^2 - 1 \right]}{\left[\left(\frac{p_{\text{in}}}{p_{\text{out}}} \right)^3 - 1 \right]} \quad (2)$$

where p_{in} is the inlet pressure.

Activity coefficients at infinite dilution of water in each IL, γ_w^∞ , were calculated with the following equation:^{58,59}

$$\ln(\gamma_w^\infty) = \ln\left(\frac{n_2 RT}{V_{Nf_w}^0}\right) - p_w^0 \left(\frac{B_{ww} - V_w^0}{RT}\right) + \left(\frac{2B_{w3} - V_w^\infty}{RT}\right) p_{out} \quad (3)$$

where n_2 is the number of moles of stationary phase component within the column, R is the ideal gas constant, T is the oven temperature, B_{ww} is the second virial coefficient of the solute in the vapor state at temperature T , B_{w3} is the mutual virial coefficient between water and the carrier gas (helium, denoted by “3”), and p_w^0 is the probe’s vapor pressure at temperature T . The values of p_w^0 result from correlated experimental data. The molar volume of the water, V_w^0 , was determined from experimental densities, and the partial molar volumes of the water at infinite dilution, V_w^∞ , were assumed to be equal to V_w^0 . The values required for the calculation of these parameters were taken from previous works.⁶⁰

Degree of Dissociation. The degree of dissociation of the $[C_4C_1im]Br$ and $[C_4C_1im]Cl$ aqueous mixtures was determined through electrical conductivity with a Mettler Toledo S47 SevenMultiTM dual meter pH/conductivity, coupled with an InLab741 Conductivity Probe as electrode. Aqueous solutions of $[C_4C_1im]Br$ and $[C_4C_1im]Cl$ with concentration ranging between 0.5 and 2.5 mol·L⁻¹ were prepared and used to measure the electrical conductivities (cf. Supporting Information). Finally, the degree of dissociation was determined using the following equation:

$$\alpha = \frac{\Lambda}{\Lambda_0} \quad (4)$$

where Λ is the molar conductivity and Λ_0 is the molar conductivity at infinite dilution. The molar conductivity at infinite dilution was extrapolated through the representation of molar conductivity in function of IL concentration.

Thermodynamic Modeling. PC-SAFT. In this work, PC-SAFT^{61,62} was applied to describe experimental pure-IL and water + IL mixture data. The PC-SAFT EoS is based on the first-order thermodynamic perturbation theory^{63–66} that uses a system of freely jointed hard spheres as reference, designated as hard-chain system. PC-SAFT, as other SAFT approaches, is especially suited to treat chain molecules, and it is hence appropriate to consider IL systems.

In PC-SAFT the dimensionless residual Helmholtz energy, a^{res} , is defined as

$$a^{res} = a^{hc} + a^{disp} + a^{assoc} + a^{polar} \quad (5)$$

where the superscripts refer to the terms accounting for the residual, hard-chain fluid, dispersive, associative, and polar interactions, respectively. The polar term was not considered in this work as previous studies reported that the polar term has only a slight influence on the PC-SAFT description of IL systems, even for non-negligible dipole moments.⁶⁷

In PC-SAFT, a nonassociating component i is provided with three pure-component parameters, namely the segment number, m_i^{seg} , the segment diameter, σ_i , and the van der Waals interaction (dispersion) energy parameter between two segments, u_i/k_B , in which k_B is the Boltzmann constant. For associating molecules, PC-SAFT requires two additional parameters, which are the association-energy parameter, $\epsilon^{A,B_i}/k_B$, and the association-volume parameter, k^{A,B_i} . For each IL two association sites (the 2B association scheme) were applied.⁶⁸

The conventional Lorenz–Berthelot combining rules are used for mixtures and described according to

$$\sigma_{ij} = \frac{1}{2}(\sigma_i + \sigma_j) \quad (6)$$

$$u_{ij} = \sqrt{u_i u_j} (1 - k_{ij}) \quad (7)$$

where k_{ij} is a binary parameter between two components i and j for the correction of the cross-dispersion energy. In this work, the ILs were considered to be present as ion pairs and thus dispersion among IL molecules was taken into account. In contrast, charge–charge interactions among the ILs were neglected.

Simple combining rules for cross-association interactions between two substances were suggested by Wolbach and Sandler⁶⁹ and used in this work:

$$\epsilon^{A,B_j} = \frac{1}{2}(\epsilon^{A,B_i} + \epsilon^{A_j,B_j}) \quad (8)$$

$$k^{A,B_j} = \sqrt{k^{A_i,B_i} k^{A_j,B_j}} \left(\frac{\sqrt{\sigma_i \sigma_j}}{\frac{1}{2}(\sigma_i + \sigma_j)} \right)^3 \quad (9)$$

Calculation of Activity Coefficients and VLE with PC-SAFT.

The water activity coefficient, γ_w , is the ratio of the water fugacity coefficient, ϕ_w^L , at the mole fraction x_w in a mixture, and the fugacity coefficient of the pure water, ϕ_{0w}^L :

$$\gamma_w(T, p, x_w) = \frac{\phi_w^L(T, p, x_w)}{\phi_{0w}^L(T, p, x_w = 1)} \quad (10)$$

where T and p represent a fixed temperature and pressure, respectively. The water fugacity coefficients can be calculated with PC-SAFT, and the exact relationship is given elsewhere.⁷⁰

The water activity coefficient at infinite dilution is calculated using the following equation:

$$\gamma_w^\infty(T, p, x_w) = \frac{\phi_w^{\infty,L}(T, p, x_w \rightarrow 0)}{\phi_{0w}^L(T, p, x_w = 1)} \quad (11)$$

where $\phi_w^{\infty,L}$ is the water fugacity coefficient at infinite dilution, which can be determined using PC-SAFT.

RESULTS AND DISCUSSION

Experimental Results. The boiling temperatures of seven water + IL systems were measured at three different pressures (0.05, 0.07, and 0.1 MPa) in a broad composition range using a microbullimometer designed by us for studying IL mixtures and previously validated and described elsewhere.⁴³ For the systems studied here, only the binary mixture formed by water + $[C_4C_1im][CF_3SO_3]$ was previously reported by Orchillés et al.⁷¹ A good agreement between our data and literature was observed with an average relative deviation, ARD (eq 15), between the two data sets, of only 0.22%. The boiling temperatures of the water + $[C_2C_1im]Cl$ system used in this work were previously reported.⁴³

The experimental VLE data for the systems measured in this work at 0.05, 0.07, and 0.1 MPa are listed in Tables S4–S10 in Supporting Information. The results obtained at 0.1 MPa are depicted in Figure 2. The data show that all the ILs studied increase the boiling temperature of the related aqueous mixtures in different extents. The influence of ILs through the boiling temperatures follows the order: $[C_4C_1im][CF_3SO_3]$

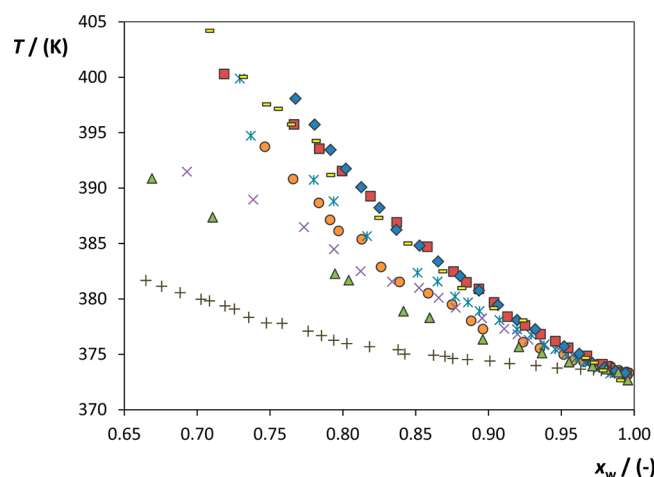


Figure 2. Experimental VLE in binary solutions of water + IL at 0.1 MPa: $[\text{C}_4\text{C}_1\text{im}][\text{CF}_3\text{SO}_3]$ (+), $[\text{C}_4\text{C}_1\text{im}][\text{SCN}]$ (green triangle), $[\text{C}_4\text{C}_1\text{im}][\text{CF}_3\text{CO}_2]$ (x), $[\text{C}_4\text{C}_1\text{im}][\text{TOS}]$ (orange circle), $[\text{C}_4\text{C}_1\text{im}]\text{Br}$ (blue asterisk), $[\text{C}_4\text{C}_1\text{im}]\text{Cl}$ (yellow rectangle), $[\text{C}_4\text{C}_1\text{im}][\text{C}_1\text{SO}_3]$ (red square), and $[\text{C}_4\text{C}_1\text{im}][\text{C}_1\text{CO}_2]$ (blue diamond).

$< [\text{C}_4\text{C}_1\text{im}][\text{SCN}] < [\text{C}_4\text{mim}][\text{CF}_3\text{CO}_2] < [\text{C}_4\text{C}_1\text{im}][\text{TOS}] < [\text{C}_4\text{C}_1\text{im}]\text{Br} < [\text{C}_4\text{C}_1\text{im}]\text{Cl} < [\text{C}_4\text{C}_1\text{im}][\text{C}_1\text{SO}_3] < [\text{C}_4\text{C}_1\text{im}][\text{C}_1\text{CO}_2]$. Since all the ILs studied have a common cation, the observed differentiation is essentially related to the effect of the anion on the water–IL interaction. In fact, a close agreement was identified between the IL's ability to increase the boiling temperature of water + IL binary solutions, and their hydrogen-bond basicity values determined by solvatochromic probes.⁷² ILs with higher hydrogen-bond basicity values interact more strongly with water and stronger IL–water interactions difficult the evaporation of the water molecules, yielding thus higher boiling-point elevations and vapor pressure depressions. The observed behavior is in agreement with previous VLE data by Zhao et al.⁴¹ and by Heym et al.¹² The researchers^{12,41} found that the ILs with higher ionic hydration ability cause a higher boiling-point elevation than other solutes, such as glycols. As an example, it can be observed in Figure 2, that the boiling-point elevation observed for a water mole fraction of 0.72 is ca. 6.2 K for $[\text{C}_4\text{C}_1\text{im}][\text{CF}_3\text{SO}_3]$ and 27.2 K for $[\text{C}_4\text{C}_1\text{im}][\text{C}_1\text{SO}_3]$. The fluorination of the methanesulfonate anion is responsible for this effect, supported by the fact that fluorinated anions are only able to form weak hydrogen bonds with water.⁷³ This effect can also be observed by comparing the boiling temperature elevation caused by ILs containing the anion acetate with trifluoroacetate where the same trend was observed.

From Figure 2 it is also visible that the boiling-point elevation increases almost linearly for those ILs that weakly interact (low boiling-point elevations) with water, namely $[\text{C}_4\text{C}_1\text{im}][\text{CF}_3\text{SO}_3]$ and $[\text{C}_4\text{C}_1\text{im}][\text{SCN}]$. In contrast, ILs such as $[\text{C}_4\text{C}_1\text{im}][\text{C}_1\text{SO}_3]$ and $[\text{C}_4\text{C}_1\text{im}][\text{C}_1\text{CO}_2]$, which present stronger interactions with water by hydrogen-bonding (high boiling-point elevation), display a nonlinear boiling-point elevation.

Figures 3 and 4 depict the VLE of several water + IL systems as a function of composition and pressure. It can be seen that pressure does not have a strong influence on the concentration-dependence of the boiling-point elevations as the T – x curves at different pressures are almost parallel to each other.

It is well-known that the volatility of an aprotic IL is negligible, and thus, the vapor phase of a binary mixture containing an IL and a molecular and volatile solvent is only constituted by the

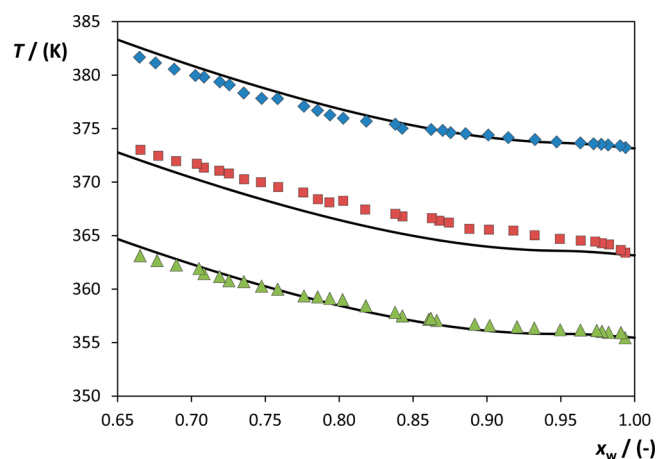


Figure 3. Experimental VLE data for the water + $[\text{C}_4\text{C}_1\text{im}][\text{CF}_3\text{SO}_3]$ system at 0.1 (blue diamond), 0.07 (red square), and 0.05 (green triangle) MPa. PC-SAFT correlation results are presented by the solid lines, and parameters values can be found in Table 1.

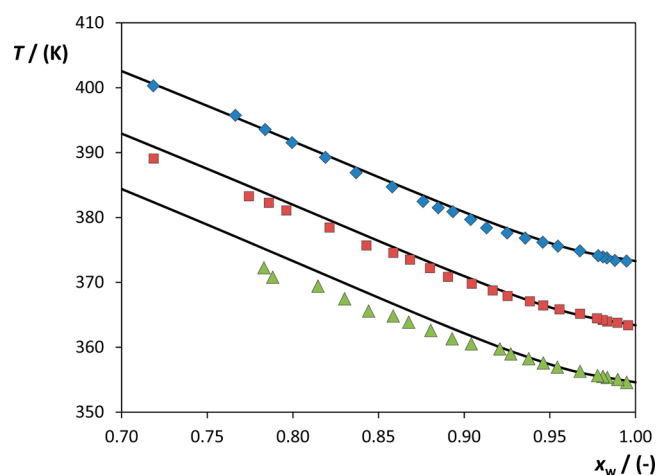


Figure 4. Experimental VLE data for water + $[\text{C}_4\text{C}_1\text{im}][\text{C}_1\text{SO}_3]$ system at 0.1 (blue diamond), 0.07 (red square), and 0.05 (green triangle) MPa. PC-SAFT correlation results are presented by the solid lines, and parameters values can be found in Table 1.

latter. Moreover, at the pressure and temperatures studied, the vapor phase fugacity coefficients are very close to unity for the compounds studied, and therefore, eq 10 can be simplified to

$$\gamma_w = \frac{p}{x_w p_w^\sigma} \quad (12)$$

where p is the system total pressure, x_i the mole fraction of the liquid phase and p_w^σ is the water vapor pressure.^{74,75} Using eq 12, the water activity coefficients can be estimated and are presented in Figure 5 at 0.1 MPa.

Negative deviation to the ideal, which translates into activity coefficients lower than unity, results from the stronger IL–water interactions than the water–water. These stronger interactions force to retain the water molecules in the liquid phase, and higher potential is required to transfer water molecules into the vapor phase. Thus, the water boiling temperature will increase as observed in the VLE experimental data. Moreover, this effect is stronger for the ILs with higher interactions with water (higher hydrogen-bond basicity). In fact, the same trend observed before for the VLE is observed for the water activity coefficients: $[\text{C}_4\text{C}_1\text{im}][\text{CF}_3\text{SO}_3] < [\text{C}_4\text{C}_1\text{im}]-$

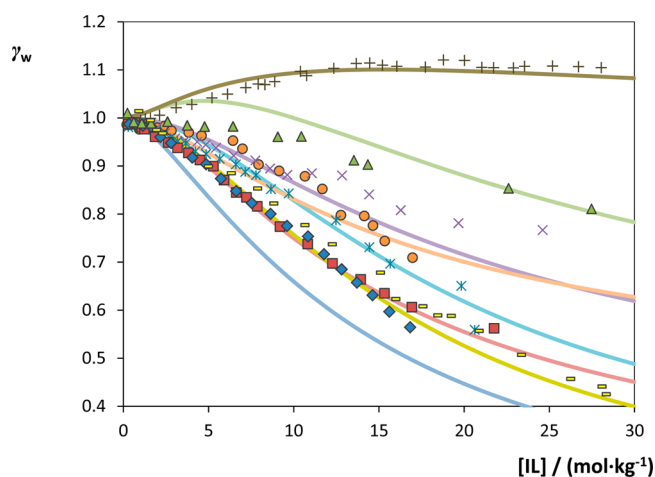


Figure 5. Water activity coefficients, γ_w , as function of the IL molality in binary solutions of water + IL at 0.1 MPa: $[C_4C_1im][CF_3SO_3]$ (+), $[C_4C_1im][SCN]$ (green triangle), $[C_4C_1im][CF_3CO_2]$ (\times), $[C_4C_1im][TOS]$ (orange circle), $[C_4C_1im]Br$ (blue asterisk), $[C_4C_1im]Cl$ (yellow rectangle), $[C_4C_1im][C_1SO_3]$ (red square), and $[C_4C_1im][C_1CO_2]$ (blue diamond). PC-SAFT correlation results are presented by the solid lines and parameters values can be found in Table 1.

$[SCN] < [C_4mim][CF_3CO_2] \approx [C_4C_1im][TOS] < [C_4C_1im]Br < [C_4C_1im]Cl < [C_4C_1im][C_1SO_3] < [C_4C_1im][C_1CO_2]$.

The water activity coefficient may be related with the solvent hydrophobicity.⁷⁶ All the studied ILs are considered hydrophilic since they are fully water-soluble. However, their hydrophilicity is not the same. For ILs with pronounced hydrophilic character (for example, $[C_4C_1im][C_1CO_2]$ and $[C_4C_1im][C_1SO_3]$) the interactions between IL and water are very strong resulting in very low water activity coefficients. In general, the less hydrophilic the IL the higher is the water activity coefficient. On the other hand, for the ILs with the weakest hydrophilic character ($[C_4C_1im][CF_3SO_3]$ and $[C_4C_1im][SCN]$), the water activity coefficients are slightly positive at low IL concentrations reflecting the weaker IL–water interaction. The influence of ions in an aqueous system is usually well described by the Hofmeister series or their ability to form hydration complexes.⁷⁷ ILs with higher affinity for water, that is, ILs with a higher charge density or higher propensity to form hydration complexes tend to the salting-out regime. The trend observed for the water activity coefficients is also in good agreement with the Hofmeister series⁷⁸ or their ability rank to interact with water by hydrogen-bonding, as expected. In fact, the observed trend correlates well with previous data where the influence of the IL anion to be salted-out by an inorganic salt was analyzed.⁷⁹ ILs with higher affinity for water are less prone for phase separation in aqueous media.⁷⁹

An irregular behavior was observed for the ILs $[C_4C_1im]Br$ and $[C_4C_1im]Cl$. The water activity coefficients on $[C_4C_1im]Br$ and $[C_4C_1im]Cl$ are opposite to the observed for the chloride and bromide common salt–water systems.^{80,81} Nevertheless, considering the Gibbs energy of ion hydration (ΔG_{hyd}) for both Br^- and Cl^- anions the Cl^- is expected to have a higher interaction with water, since it presents a lower ΔG value ($\Delta G_{hyd}(Br^-) = -321 \text{ kJ} \cdot \text{mol}^{-1}$ and $\Delta G_{hyd}(Cl^-) = -347 \text{ kJ} \cdot \text{mol}^{-1}$),⁸² which is in agreement with the results obtained in this work for the water activity coefficients. Moreover, at the very high IL concentrations that are studied in this work the formation of ion pairs can occur,⁸³ causing a lower IL

interaction with water. This phenomenon can be observed and quantified through the degree of dissociation represented in Figure 6 for both $[C_4C_1im]Br$ and $[C_4C_1im]Cl$.

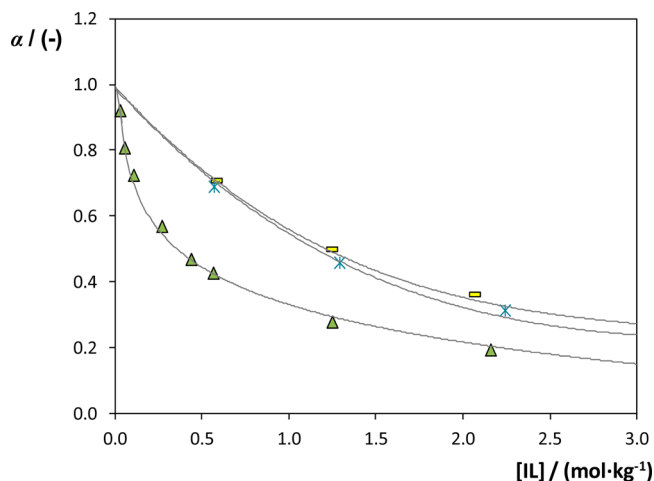


Figure 6. Degree of dissociation, α , as function of the IL molality in binary solutions of water + IL at 298.15 K and atmospheric pressure: $[C_4C_1im][SCN]$ (green triangle), $[C_4C_1im]Br$ (blue asterisk), and $[C_4C_1im]Cl$ (yellow rectangle).

At $2 \text{ mol} \cdot \text{kg}^{-1}$ the degree of dissociation is 0.336 for $[C_4C_1im]Br$ and 0.361 for $[C_4C_1im]Cl$. As expected, due to the similarities in structure and size of the ions composing these compounds, the differences observed between both ILs degree of dissociation are not very large. However, the differences observed are in agreement with the results obtained in this work for the water activity coefficients. $[C_4C_1im]Cl$ has a higher dissociation degree consequently meaning a higher interaction with water.

Held et al.⁸⁴ reported a similar behavior in the water activity coefficients of aqueous solutions of electrolytes containing the anions hydroxides, fluorides, and acetates. For these salts, the water activity coefficients presented a reverse sequence compared to the alkali salts trend. This behavior was justified by the possibility of occurring a localized hydrolysis⁸⁵ in presence of anions with strong ability to accept protons, which results in the decreasing of the number of ions in the solution.

In Figure 6, it is also represented the degree of dissociation for $[C_4C_1im][SCN]$, one of the less hydrophilic ILs studied in this work. As expected, a lower degree of dissociation (0.218 at $2 \text{ mol} \cdot \text{kg}^{-1}$) compared to both $[C_4C_1im]Br$ and $[C_4C_1im]Cl$ was obtained for this IL, which is in agreement with the results obtained by Yee et al.,⁸³ showing that the tendency for dissociation decreases with the anion hydrophobicity.

Modeling Results. Ji et al.⁵⁶ and Nann et al.⁵⁵ already used PC-SAFT to model IL solutions. The authors treated ILs as molecules with a distinctive association behavior by using the 2B association scheme, where each IL was assigned two association sites, and association interaction was allowed between two different sites of two IL molecules. This approach was also applied in this work. Thus, within this framework, IL molecules can interact with each other and with water via hard-chain repulsion, dispersion, and association. Furthermore, according to the findings of Köddermann et al.,⁸⁶ the ILs were assumed to be nondissociated and nonaggregated for the PC-SAFT modeling in this work. This approach is justified through the results presented in Figure 6, where it is possible to

see that ILs only present an extensive dissociation in dilute solutions and that at the concentration range studied in this work assuming ion pairs instead of dissociated ions is an acceptable approach.

The PC-SAFT parameters for the ILs were determined by a simultaneous regression of pure-IL densities,^{87–92} water activity coefficients at 298.15 K,⁹³ and the VLE data of the water + IL binary mixtures at 0.1 MPa (determined in this work) using the following objective function:

$$\text{OF} = \sum_i^{NP} \left(\frac{\rho_i^{\text{exp}} - \rho_i^{\text{calc}}}{\rho_i^{\text{exp}}} \right)^2 + \sum_i^{NP} \left(\frac{\gamma_i^{\text{exp}} - \gamma_i^{\text{calc}}}{\gamma_i^{\text{exp}}} \right)^2 + \sum_i^{NP} \left(\frac{T_i^{b,\text{exp}} - T_i^{b,\text{calc}}}{T_i^{b,\text{exp}}} \right)^2 \quad (13)$$

All the PC-SAFT parameters for the ILs considered in this work are summarized in Table 1, including the parameters of water that were taken from literature.⁹⁴

As a result of the parameter estimation, the association-energy parameters were found to be zero for all ILs with negative deviations to ideality. Since all these ILs are strongly hydrophilic, this result may be related with the possibility of each IL molecule to be completely surrounded by water molecules and thereby hindering direct IL–IL hydrogen bonds. In contrast, for [C₄C₁im][CF₃SO₃], a nonzero association-energy parameter was obtained. [C₄C₁im][CF₃SO₃] is less hydrophilic, presenting positive deviation to ideality. The association-volume parameters seem to follow a very specific order, as presented in Table 1: [C₄C₁im][CH₃CO₂] > [C₄C₁im][CH₃SO₃] > [C₄C₁im]Cl > [C₄C₁im]Br > [C₄C₁im][TOS] > [C₄C₁im][CF₃CO₂] > [C₄C₁im][SCN] > [C₄C₁im][CF₃SO₃]. This order clearly shows that the PC-SAFT association strength is in agreement with the experimentally observed sequence of water activity coefficients, meaning that the water–IL interactions due to hydrogen bonding are correctly being taken into account within the PC-SAFT framework.

The results obtained for the segment number (m_i^{seg}) and the segment diameter (σ_i) are within reasonable ranges. The segment diameter varies between 2.75 Å for [C₄C₁im][C₁SO₃] and 3.60 Å for [C₄C₁im]Br. The segment numbers oscillate considerably with the anion that constitutes the IL. The segment number and the segment diameter parameters of the ILs depend linearly on the molecular weight (M_w) according to the following equation:

$$m_i^{\text{seg}} \sigma_i^3 = 0.582 M_w + 133.09 \text{ (\AA}^3) \quad (14)$$

The values for the dispersion-energy parameters of the ILs are also reasonable, ranging between 175.62 K for [C₄C₁im][TOS] and 447.15 K for [C₄C₁im]Br. This parameter does not depend linearly on the molecular weight.

The fitting errors of the pure-IL density, water activity coefficient, and VLE of water + IL binary mixtures are expressed as the average relative deviation (ARD) between modeled and experimental data:

$$\text{ARD} = 100 \frac{1}{NP} \sum_{k=1}^{NP} \left| \left(1 - \frac{z_k^{\text{mod}}}{z_k^{\text{exp}}} \right) \right| \quad (15)$$

where NP is the number of experimental data points and the superscripts “mod” and “exp” are the modeled results and

Table 1. PC-SAFT Parameters^a for Water and ILs, as well as ARD Values (Calculated with Equation 15), for Pure and Mixture Properties

IL	[C ₄ C ₁ im][CF ₃ SO ₃]	[C ₄ C ₁ im][SCN]	[C ₄ C ₁ im][CF ₃ CO ₂]	[C ₄ C ₁ im][TOS]	[C ₄ C ₁ im]Br	[C ₄ C ₁ im]Cl	[C ₄ C ₁ im][C ₁ SO ₃]	[C ₄ C ₁ im][C ₁ CO ₂]	water
T range ^b (K)	[293.15–393.15]	[278.15–363.15]	[278.15–338.15]	[333.15–353.15]	[293.22–373.08]	[372.66–430.10]	[298.15–373.15]	[278.15–363.15]	
x_{IL} range ^b	[0.006–0.820]	[0.010–0.969]	[0.006–0.861]	[0.004–0.335]	[0.005–0.410]	[0.012–0.415]	[0.005–0.376]	[0.006–0.961]	
σ_i (Å)	3.3037	3.0300	3.0845	3.1681	3.6000	3.5000	2.7482	2.9504	T dependent ^c
m_i^{seg}	8.1368	10.3743	9.5000	10.0000	5.6851	5.1737	12.8442	10.0000	1.2047
u_{IL} (K)	206.85	246.95	224.30	175.62	447.15	294.38	214.78	251.90	353.95
$\epsilon^{A,B}/k_B$ (K)	189.21	0.00	0.00	0.00	0.00	0.00	0.00	0.00	2425.67
$k^{A,B}$	0.144	0.548	0.600	0.700	0.800	0.844	0.950	1.000	0.045
k_{ij}	–0.0741	–0.0173	–0.0725	–0.1461	0.0354	–0.0375	–0.0827	–0.0960	
ARD % in ρ_{IL}	1.37	0.78	0.94	0.90	0.42	1.00	0.78	2.53	
ARD % in γ_w	2.59	2.97	4.61	2.20	1.61	2.52	1.59	5.28	
ARD % in VLE	1.47	2.89	3.07	2.93	2.11	3.95	1.01	7.85	

^aSegment number, m_i^{seg} , segment diameter, σ_i , dispersion energy parameter of IL, u_{IL} , association-energy parameter, $\epsilon^{A,B}/k_B$, and association-volume parameter, $k^{A,B}$. ^bRange of temperatures and IL mole fraction considering for the PC-SAFT parameters modeling. ^c $\sigma = 2.7927 + 10.11 \exp(-0.01775 \cdot T/K) - 1.417 \exp(-0.01146 \cdot T/K)$

experimental data, respectively. These values are listed in Table 1.

PC-SAFT pure-IL densities are in good agreement with the experimental data with small deviations. To give an example, the ARD values range between 0.42% for the pure-IL densities of $[\text{C}_4\text{C}_1\text{im}]\text{Br}$ and 2.53% for $[\text{C}_4\text{C}_1\text{im}][\text{C}_1\text{CO}_2]$, as depicted in Figure 7.

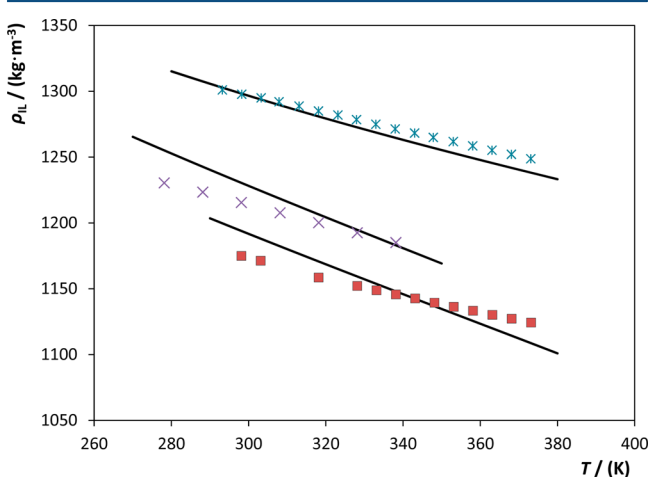


Figure 7. Experimental pure-IL density data, ρ_{IL} , as a function of temperature at atmospheric pressure: $[\text{C}_4\text{C}_1\text{im}]\text{Br}$ (blue asterisk), $[\text{C}_4\text{C}_1\text{im}][\text{CF}_3\text{CO}_2]$ (\times), $[\text{C}_4\text{C}_1\text{im}][\text{C}_1\text{SO}_3]$ (red square). PC-SAFT correlation results are presented by the solid lines and the pure compound parameters values can be found in Table 1.

The modeling results obtained with the PC-SAFT for the water + IL binary systems are presented hereafter. A temperature-independent binary interaction parameter (k_{ij}), fitted to VLE data at 0.1 MPa and water activity coefficients at 298.15 K,⁹³ was used for each binary system. Some of the results obtained are illustrated in Figure 8, where the activity coefficients are shown as function of the molality of the IL (i.e., mole of IL per kg of water solvent). It can be observed, from Figure 8, that PC-SAFT provides a good description of the

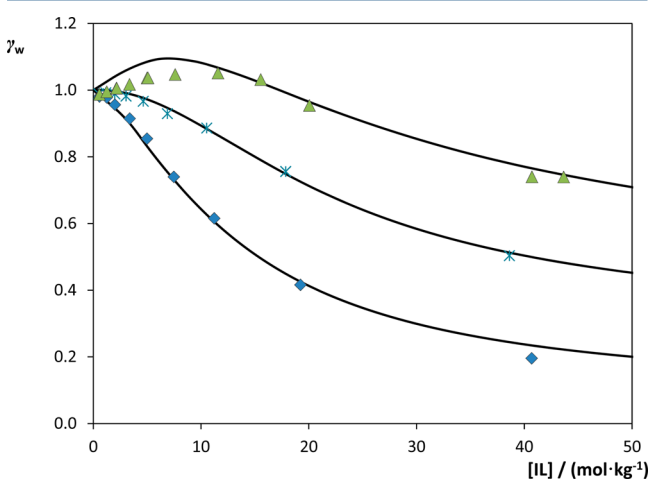


Figure 8. Experimental water activity coefficients, γ_w , at 298.15 K⁹³ as a function of the IL molality in binary solutions of water + IL at 298.15 K: $[\text{C}_4\text{C}_1\text{im}][\text{SCN}]$ (green triangle), $[\text{C}_4\text{C}_1\text{im}]\text{Br}$ (blue asterisk), $[\text{C}_4\text{C}_1\text{im}][\text{C}_1\text{CO}_2]$ (blue diamond). PC-SAFT correlation results are presented by the solid lines and parameters values can be found in Table 1.

behavior of both the more and the less hydrophobic ILs. The ARD values range between 1.59% for $[\text{C}_4\text{C}_1\text{im}][\text{C}_1\text{SO}_3]$ and 5.28% for $[\text{C}_4\text{C}_1\text{im}][\text{C}_1\text{CO}_2]$.

The PC-SAFT modeling of the VLE for the systems measured in this work are presented in Figures 3 and 4 for the ILs $[\text{C}_4\text{C}_1\text{im}][\text{CF}_3\text{SO}_3]$ and $[\text{C}_4\text{C}_1\text{im}][\text{C}_1\text{SO}_3]$, respectively. The results are in good agreement with the experimental data: 0.1 MPa with an overall ARD of 3.04%. As expected, the water activity coefficients at 0.1 MPa for the binary systems are also well described by PC-SAFT, as observed in Figure 5. It is also shown that PC-SAFT can successfully be used to predict the VLE data at 0.07 and 0.05 MPa with an overall ARD of 3.82% and 5.20%, respectively. It should be emphasized that all IL pure-component PC-SAFT parameters and binary interaction parameters are temperature independent.

Finally, PC-SAFT was applied to predict the water activity coefficients at infinite dilution in ILs. In fact, for the ILs studied in this work, the experimental data for the water activity coefficients cover very large concentration ranges in most cases. However, data at such high IL molalities are difficult (and sometimes impossible depending on the IL) to experimentally determine due to solubility, viscosity, or decomposition concerns. Thus, it is strongly desirable to have a model that is able to estimate the water activity coefficients at infinite dilution either predicting them or by extrapolation of the available data. Table 2 lists experimental water activity

Table 2. Experimental Water Activity Coefficients at Infinite Dilution and Predicted with PC-SAFT, as Well as AD and AAD Values (Calculated with Equations 16 and 17)

IL	γ_w^∞		
	experimental data	PC-SAFT	AD
$[\text{C}_4\text{C}_1\text{im}][\text{CF}_3\text{SO}_3]$	0.929 ¹⁴	1.098	0.169
$[\text{C}_4\text{C}_1\text{im}][\text{SCN}]$	0.302 ²³	0.371	0.069
$[\text{C}_4\text{C}_1\text{im}][\text{TOS}]$	0.167 ²⁸	0.288	0.121
$[\text{C}_4\text{C}_1\text{im}][\text{CF}_3\text{CO}_2]$	0.133	0.231	0.098
$[\text{C}_4\text{C}_1\text{im}]\text{Br}$	0.045	0.248	0.203
$[\text{C}_4\text{C}_1\text{im}]\text{Cl}$	0.025	0.162	0.137
$[\text{C}_4\text{C}_1\text{im}][\text{C}_1\text{SO}_3]$	0.097	0.136	0.039
$[\text{C}_4\text{C}_1\text{im}][\text{C}_1\text{CO}_2]$	0.013	0.070	0.057
AAD			0.112

coefficients at infinite dilution for the ILs under study. For those for which no data were available in literature,^{14,23,28} they were measured in this work. The absolute deviation and the average absolute deviation between the experimental data and PC-SAFT predicted values were calculated through eqs 16 and 17 and are presented in Table 2.

$$\text{AD} = |z_k^{\text{exp}} - z_k^{\text{mod}}| \quad (16)$$

$$\text{AAD} = \frac{1}{NP} \sum_{k=1}^{NP} |z_k^{\text{exp}} - z_k^{\text{mod}}| \quad (17)$$

The PC-SAFT modeling used the model parameters presented in Table 1 fitted to VLE and water activity coefficients at finite concentrations and not to activity coefficients at infinite dilution. The results appear to be quite promising as the model provides a satisfactorily prediction of the experimental water activity coefficients at infinite dilution. While PC-SAFT slightly overestimates the experimental data, the sequence of the experimental and predicted γ_w^∞ values are in good

agreement except for $[C_4C_1im]Br$ and $[C_4C_1im]Cl$. Availability of activity coefficients in a minimum concentration range seems thus to be required for an adequate prediction of the infinite dilution activity coefficients. For $[C_4C_1im]Br$ and $[C_4C_1im]Cl$, this range seems to be insufficient.

CONCLUSIONS

VLE data for seven water + imidazolium-based IL systems covering different families of anions at three different pressures were measured in this work. The results indicate that the imidazolium-based ILs studied cause boiling-point elevations of different degrees according to the interaction strengths between water and the IL that mainly depends on the nature of the IL anion.

The PC-SAFT equation of state was used for the description of the experimental data. The PC-SAFT pure-component parameters and the binary interaction parameter were determined by a simultaneous fitting to pure-IL densities, water activity coefficients at 298.15 K, and VLE data at 0.10 MPa. The binary interaction parameters were considered to be temperature independent. This set of parameters allowed for quantitative modeling the pure-IL density, water activity coefficients at 298.15 K, and the VLE at 0.10 MPa for the water + IL binary mixtures. VLE at pressures different from 0.10 MPa can be predicted reasonably with PC-SAFT by using binary interaction parameters fitted to VLE data at 0.10 MPa. Moreover, PC-SAFT is capable to satisfactorily predict water activity coefficients at infinite dilution for systems where model parameters were adjusted to water activity coefficients at low IL molalities.

ASSOCIATED CONTENT

Supporting Information

Experimental VLE data for the water + IL systems at 0.1, 0.07, and 0.05 MPa; experimental electrical conductivity data for water + IL systems at 298.15 K and atmospheric pressure. This material is available free of charge via the Internet at <http://pubs.acs.org>.

AUTHOR INFORMATION

Corresponding Authors

*Tel: +351 234370200. Fax: +351 234370084. E-mail: jcoutinho@ua.pt.

*Tel: +49231 7552086. Fax +49231 7552572. E-mail: christoph.held@bci.tu-dortmund.de.

Author Contributions

[†]H.P. and I.K. contributed equally.

Notes

The authors declare no competing financial interest.

ACKNOWLEDGMENTS

The authors are grateful for financial support from FCT—Fundação para a Ciência e a Tecnologia—for the projects PTDC/QUI-QUI/121520/2010 and Pest-C/CTM/LA0011/2013 and postdoctoral and doctoral grants SFRH/BPD/71200/2010, SFRH/BPD/76850/2011, and SFRH/BD/85248/2012 to M.B. Oliveira, I. Khan, and H. Passos, respectively.

REFERENCES

(1) Liang, S.; Chen, W.; Cheng, K.; Guo, Y.; Gui, X. The Latent Application of Ionic Liquids in Absorption Refrigeration. In

Applications of Ionic Liquids in Science and Technology; Handy, P. S., Eds.; InTech: Croatia, 2011; pp 467–494.

(2) Zhuo, C. Z.; Machielsen, C. H. M. Thermophysical Properties of the Trifluoroethanol–Pyrrolidone System for Absorption Heat Transformers. *Int. J. Refrig.* **1993**, *16*, 357–363.

(3) Tufano, V. Simplified Criteria for the Development of New Absorption Working Pairs. *Appl. Therm. Eng.* **1998**, *18*, 171–177.

(4) Zheng, D.; Ji, P.; Qi, J. Maximum Excess Gibbs Function of Working Pairs and Absorption Cycle Performance. *Int. J. Refrig.* **2001**, *24*, 834–840.

(5) Kernen, M.; Lee, L. L.; Perez-Blanco, H. A Study of Solution Properties to Optimize Absorption Cycle COP. *Int. J. Refrig.* **1995**, *18*, 42–50.

(6) Sriksirin, P.; Aphornratana, S.; Chungpaibulpatana, S. A Review of Absorption Refrigeration Technologies. *Renewable Sustainable Energy Rev.* **2001**, *5*, 343–372.

(7) Yokozeki, A.; Shiflett, M. B. Binary and Ternary Phase Diagrams of Benzene, Hexafluorobenzene, and Ionic Liquid $[emim][Tf_2N]$ Using Equations of State. *Ind. Eng. Chem. Res.* **2008**, *47*, 8389–8395.

(8) Zuo, G.; Zhao, Z.; Yan, S.; Zhang, X. Thermodynamic Properties of a New Working Pair: 1-Ethyl-3-methylimidazolium Ethylsulfate and Water. *Chem. Eng. J.* **2010**, *156*, 613–617.

(9) Zhang, X.; Hu, D. Performance Analysis of the Single-Stage Absorption Heat Transformer using a New Working Pair Composed of Ionic Liquid and Water. *Appl. Therm. Eng.* **2012**, *37*, 129–135.

(10) Nie, N.; Zheng, D.; Dong, L.; Li, Y. Thermodynamic Properties of the Water + 1-(2-Hydroxyethyl)-3-methylimidazolium Chloride System. *J. Chem. Eng. Data* **2012**, *57*, 3598–3603.

(11) Dong, L.; Zheng, D.; Nie, N.; Li, Y. Performance Prediction of Absorption Refrigeration Cycle based on the Measurements of Vapor Pressure and Heat Capacity of $H_2O + [DMIM]DMP$ System. *Appl. Energy* **2012**, *98*, 326–332.

(12) Heym, F.; Haber, J.; Korth, W.; Etsold, B. J. M.; Jess, A. Vapor Pressure of Water in Mixtures with Hydrophilic Ionic Liquids—A Contribution to the Design of Processes for Drying of Gases by Absorption in Ionic Liquids. *Chem. Eng. Technol.* **2010**, *33*, 1625–1634.

(13) Domańska, U.; Marciniak, A. Activity Coefficients at Infinite Dilution Measurements for Organic Solutes and Water in the Ionic Liquid 1-Ethyl-3-methylimidazolium Trifluoroacetate. *J. Phys. Chem. B* **2007**, *111*, 11984–11988.

(14) Domańska, U.; Marciniak, A. Activity Coefficients at Infinite Dilution Measurements for Organic Solutes and Water in the Ionic Liquid 1-Butyl-3-methylimidazolium Trifluoromethanesulfonate. *J. Phys. Chem. B* **2008**, *112*, 11100–11105.

(15) Domańska, U.; Marciniak, A. Measurements of Activity Coefficients at Infinite Dilution of Aromatic and Aliphatic Hydrocarbons, Alcohols, and Water in the new Ionic Liquid $[EMIM][SCN]$ using GLC. *J. Chem. Thermodyn.* **2008**, *40*, 860–866.

(16) Krummen, M.; Wasserscheid, P.; Gmehling, J. Measurement of Activity Coefficients at Infinite Dilution in Ionic Liquids using the Dilutor Technique. *J. Chem. Eng. Data* **2002**, *47*, 1411–1417.

(17) Diedenhofen, M.; Eckert, F.; Klamt, A. Prediction of Infinite Dilution Activity Coefficients of Organic Compounds in Ionic Liquids using COSMO-RS. *J. Chem. Eng. Data* **2003**, *48*, 475–479.

(18) Ge, M.; Xiong, J.; Wang, L. Theoretical Prediction for the Infinite Dilution Activity Coefficients of Organic Compounds in Ionic Liquids. *Chin. Sci. Bull.* **2009**, *54*, 2225–2229.

(19) Domańska, U.; Królikowski, M. Measurements of Activity Coefficients at Infinite Dilution for Organic Solutes and Water in the Ionic Liquid 1-Ethyl-3-methylimidazolium Methanesulfonate. *J. Chem. Thermodyn.* **2012**, *54*, 20–27.

(20) Kato, R.; Gmehling, J. Systems with Ionic Liquids: Measurement of VLE and γ^∞ Data and Prediction of their Thermodynamic Behavior using Original UNIFAC, mod. UNIFAC(Do) and COSMO-RS(OI). *J. Chem. Thermodyn.* **2005**, *37*, 603–619.

(21) Kato, R.; Gmehling, J. Activity Coefficients at Infinite Dilution of Various Solutes in the Ionic Liquids $[MMIM]^+[CH_3SO_4]^-$, $[MMIM]^+[CH_3OC_2H_4SO_4]^-$, $[MMIM]^+[(CH_3)_2PO_4]^-$,

$[C_5H_5NC_2H_5]^+[(CF_3SO_2)_2N]^-$, and $[C_5H_5NH]^+[C_2H_5OC_2H_4OSO_3]^-$. *Fluid Phase Equilib.* **2004**, *226*, 37–44.

(22) Domańska, U.; Redhi, G. G.; Marciniak, A. Activity Coefficients at Infinite Dilution Measurements for Organic Solutes and Water in the Ionic Liquid 1-Butyl-1-Methylpyrrolidinium Trifluoromethanesulfonate using GLC. *Fluid Phase Equilib.* **2009**, *278*, 97–102.

(23) Domańska, U.; Laskowska, M. Erratum: "Measurements of Activity Coefficients at Infinite Dilution of Aliphatic and Aromatic Hydrocarbons, Alcohols, Thiophene, Tetrahydrofuran, MTBE, and Water in Ionic Liquid [BMIM][SCN] using GLC" [*J. Chem. Thermodyn.* **41** (2009) 645–650]. *J. Chem. Thermodyn.* **2010**, *42*, 947–948.

(24) Domańska, U.; Marciniak, A.; Królikowska, M.; Arasimowicz, M. Activity Coefficients at Infinite Dilution Measurements for Organic Solutes and Water in the Ionic Liquid 1-Hexyl-3-methylimidazolium Thiocyanate. *J. Chem. Eng. Data* **2010**, *55*, 2532–2536.

(25) Domańska, U.; Królikowski, M.; Acree, W. E., Jr Thermodynamics and Activity Coefficients at Infinite Dilution Measurements for Organic Solutes and Water in the Ionic Liquid 1-Butyl-1-methylpyrrolidinium Tetracyanoborate. *J. Chem. Thermodyn.* **2011**, *43*, 1810–1817.

(26) Domańska, U.; Królikowska, M.; Acree, W. E., Jr; Baker, G. A. Activity Coefficients at Infinite Dilution Measurements for Organic Solutes and Water in the Ionic Liquid 1-Ethyl-3-methylimidazolium Tetracyanoborate. *J. Chem. Thermodyn.* **2011**, *43*, 1050–1057.

(27) Domańska, U.; Lukoshko, E. V.; Wlazło, M. Measurements of Activity Coefficients at Infinite Dilution for Organic Solutes and Water in the Ionic Liquid 1-Hexyl-3-methylimidazolium Tetracyanoborate. *J. Chem. Thermodyn.* **2012**, *47*, 389–396.

(28) Domańska, U.; Królikowski, M. Determination of Activity Coefficients at Infinite Dilution of 35 Solutes in the Ionic Liquid, 1-Butyl-3-methylimidazolium Tosylate, Using Gas–Liquid Chromatography. *J. Chem. Eng. Data* **2010**, *55*, 4817–4822.

(29) Domańska, U.; Królikowska, M. Measurements of Activity Coefficients at Infinite Dilution for Organic Solutes and Water in the Ionic Liquid 1-Butyl-1-methylpiperidinium Thiocyanate. *J. Chem. Eng. Data* **2010**, *56*, 124–129.

(30) Domańska, U.; Marciniak, A. Physicochemical Properties and Activity Coefficients at Infinite Dilution for Organic Solutes and Water in the Ionic Liquid 1-Decyl-3-methylimidazolium Tetracyanoborate. *J. Phys. Chem. B* **2010**, *114*, 16542–16547.

(31) Domańska, U.; Królikowski, M. Thermodynamics and Activity Coefficients at Infinite Dilution Measurements for Organic Solutes and Water in the Ionic Liquid *n*-Hexyl-3-methylpyridinium Tosylate. *J. Phys. Chem. B* **2011**, *115*, 7397–7404.

(32) Marciniak, A.; Wlazło, M. Activity Coefficients at Infinite Dilution and Physicochemical Properties for Organic Solutes and Water in the Ionic Liquid 1-(2-Methoxyethyl)-1-methylpiperidinium Trifluorotris(perfluoroethyl)phosphate. *J. Chem. Thermodyn.* **2013**, *57*, 197–202.

(33) Wlazło, M.; Marciniak, A. Activity Coefficients at Infinite Dilution and Physicochemical Properties for Organic Solutes and Water in the Ionic Liquid 4-(2-Methoxyethyl)-4-methylmorpholinium Trifluorotris(perfluoroethyl)phosphate. *J. Chem. Thermodyn.* **2012**, *54*, 366–372.

(34) Marciniak, A.; Wlazło, M. Activity Coefficients at Infinite Dilution and Physicochemical Properties for Organic Solutes and Water in the Ionic Liquid 1-(2-Methoxyethyl)-1-methylpyrrolidinium Bis(trifluoromethylsulfonyl)-amide. *J. Chem. Thermodyn.* **2012**, *54*, 90–96.

(35) Yokozeki, A.; Shiflett, M. B. Water Solubility in Ionic Liquids and Application to Absorption Cycles. *Ind. Eng. Chem. Res.* **2010**, *49*, 9496–9503.

(36) Wang, J.; Zheng, D.; Fan, L.; Dong, L. Vapor Pressure Measurement for the Water + 1,3-Dimethylimidazolium Chloride System and 2,2,2-Trifluoroethanol + 1-Ethyl-3-methylimidazolium Tetrafluoroborate System. *J. Chem. Eng. Data* **2010**, *55*, 2128–2132.

(37) Kim, Y. J.; Kim, S.; Joshi, Y. K.; Fedorov, A. G.; Kohl, P. A. Thermodynamic Analysis of an Absorption Refrigeration System with Ionic-Liquid/Refrigerant Mixture as a Working Fluid. *Energy* **2012**, *44*, 1005–1016.

(38) Wu, X.; Li, J.; Fan, L.; Zheng, D.; Dong, L. Vapor Pressure Measurement of Water + 1,3-Dimethylimidazolium Tetrafluoroborate System. *Chin. J. Chem. Eng.* **2011**, *19*, 473–477.

(39) Kim, K.-S.; Park, S.-Y.; Choi, S.; Lee, H. Vapor Pressures of the 1-Butyl-3-methylimidazolium Bromide + Water, 1-Butyl-3-methylimidazolium Tetrafluoroborate + Water, and 1-(2-Hydroxyethyl)-3-methylimidazolium Tetrafluoroborate + Water Systems. *J. Chem. Eng. Data* **2004**, *49*, 1550–1553.

(40) Jiang, X.-C.; Wang, J.-F.; Li, C.-X.; Wang, L.-M.; Wang, Z.-H. Vapor Pressure Measurement for Binary and Ternary Systems Containing Water Methanol Ethanol and an Ionic Liquid 1-Ethyl-3-methylimidazolium Diethylphosphate. *J. Chem. Thermodyn.* **2007**, *39*, 841–846.

(41) Zhao, J.; Jiang, X.-C.; Li, C.-X.; Wang, Z.-H. Vapor Pressure Measurement for Binary and Ternary Systems Containing a Phosphoric Ionic Liquid. *Fluid Phase Equilib.* **2006**, *247*, 190–198.

(42) Wang, J.-F.; Li, C.-X.; Wang, Z.-H.; Li, Z.-J.; Jiang, Y.-B. Vapor Pressure Measurement for Water, Methanol, Ethanol, and Their Binary Mixtures in the Presence of an Ionic Liquid 1-Ethyl-3-methylimidazolium Dimethylphosphate. *Fluid Phase Equilib.* **2007**, *255*, 186–192.

(43) Carvalho, P. J.; Khan, I.; Morais, A.; Granjo, J. F. O.; Oliveira, N. M. C.; Santos, L. M. N. B. F.; Coutinho, J. A. P. A New Microbullimeter for the Measurement of the Vapor Liquid Equilibrium of Ionic Liquid Systems. *Fluid Phase Equilib.* **2013**, *354*, 156–165.

(44) Domańska, U.; Marciniak, A. Phase Behavior of 1-Hexyloxymethyl-3-methylimidazolium and 1,3-Dihexyloxymethyl-imidazolium Based Ionic Liquids with Alcohols, Water, Ketones, and Hydrocarbons: The Effect of Cation and Anion on Solubility. *Fluid Phase Equilib.* **2007**, *260*, 9–18.

(45) Nebig, S.; Böltz, R.; Gmehling, J. Measurement of Vapor–Liquid Equilibria (VLE) and Excess Enthalpies (HE) of Binary Systems with 1-Alkyl-3-methylimidazolium Bis(trifluoromethylsulfonyl)imide and Prediction of these Properties and γ_{∞} Using Modified UNIFAC (Dortmund). *Fluid Phase Equilib.* **2007**, *258*, 168–178.

(46) Li, J.; He, C.; Peng, C.; Liu, H.; Hu, Y.; Paricaud, P. Modeling of the Thermodynamic Properties of Aqueous Ionic Liquid Solutions with an Equation of State for Square-well Chain Fluid with Variable Range. *Ind. Eng. Chem. Res.* **2011**, *50*, 7027–7040.

(47) Wang, T.; Peng, C.; Liu, H.; Hu, Y.; Jiang, J. Equation of State for the Vapor–Liquid Equilibria of Binary Systems Containing Imidazolium-Based Ionic Liquids. *Ind. Eng. Chem. Res.* **2007**, *46*, 4323–4329.

(48) Banerjee, T.; Singh, M. K.; Khanna, A. Prediction of Binary VLE for Imidazolium Based Ionic Liquid Systems Using COSMO-RS. *Ind. Eng. Chem. Res.* **2006**, *45*, 3207–3219.

(49) Freire, M. G.; Neves, C. M. S. S.; Carvalho, P. J.; Gardas, R. L.; Fernandes, A. M.; Marrucho, I. M.; Santos, L. M. N. B. F.; Coutinho, J. A. P. Mutual Solubilities of Water and Hydrophobic Ionic Liquids. *J. Phys. Chem. B* **2007**, *111*, 13082–13089.

(50) Freire, M. G.; Ventura, S. P. M.; Santos, L. M. N. B. F.; Marrucho, I. M.; Coutinho, J. A. P. Evaluation of COSMO-RS for the Prediction of LLE and VLE of Water and Ionic Liquids Binary Systems. *Fluid Phase Equilib.* **2008**, *268*, 74–84.

(51) Freire, M. G.; Carvalho, P. J.; Gardas, R. L.; Santos, L. M. N. B. F.; Marrucho, I. M.; Coutinho, J. A. P. Solubility of Water in Tetradecyltriethylphosphonium-Based Ionic Liquids. *J. Chem. Eng. Data* **2008**, *53*, 2378–2382.

(52) Llovel, F.; Valente, E.; Vilaseca, O.; Vega, L. F. Modeling Complex Associating Mixtures with $[C_n\text{-mim}][Tf_2N]$ Ionic Liquids: Predictions from the soft-SAFT Equation. *J. Phys. Chem. B* **2011**, *115*, 4387–4398.

- (53) Vega, L. F.; Vilaseca, O.; Llovel, F.; Andreu, J. S. Modeling Ionic Liquids and the Solubility of Gases in Them: Recent Advances and Perspectives. *Fluid Phase Equilib.* **2010**, *294*, 15–30.
- (54) Padaszyński, K.; Domańska, U. Thermodynamic Modeling of Ionic Liquid Systems: Development and Detailed Overview of Novel Methodology Based on the PC-SAFT. *J. Phys. Chem. B* **2012**, *116*, 5002–5018.
- (55) Nann, A.; Mündges, J.; Held, C.; Verevkin, S. P.; Sadowski, G. Molecular Interactions in 1-Butanol + IL Solutions by Measuring and Modeling Activity Coefficients. *J. Phys. Chem. B* **2013**, *117*, 3173–3185.
- (56) Ji, X.; Held, C.; Sadowski, G. Modeling Imidazolium-Based Ionic Liquids with ePC-SAFT. *Fluid Phase Equilib.* **2012**, *335*, 64–73.
- (57) Dong, L.; Zheng, D. X.; Wei, Z.; Wu, X. H. Synthesis of 1,3-Dimethylimidazolium Chloride and Volumetric Property Investigations of its Aqueous Solution. *Int. J. Thermophys* **2009**, *30*, 1480–1490.
- (58) Cruickshank, A. J. B.; Windsor, M. L.; Young, C. L. The Use of Gas–Liquid Chromatography to Determine Activity Coefficients and Second Virial Coefficients of Mixtures. I. Theory and Verification of Method of Data Analysis. *Proc. R. Soc. London, Ser. A* **1966**, *295*, 259–270.
- (59) Cruickshank, A. J. B.; Windsor, M. L.; Young, C. L. The Use of Gas–Liquid Chromatography to Determine Activity Coefficients and Second Virial Coefficients of Mixtures. II. Experimental Studies on Hydrocarbon Solutes. *Proc. R. Soc. London, Ser. A* **1966**, *295*, 271–287.
- (60) Revelli, A.-L.; Sprunger, L. M.; Gibbs, J.; Acree, W. E.; Baker, G. A.; Mutelet, F. Activity Coefficients at Infinite Dilution of Organic Compounds in Trihexyl(tetradecyl)phosphonium Bis-(trifluoromethylsulfonyle)imide using Inverse Gas Chromatography. *J. Chem. Eng. Data* **2009**, *54*, 977–985.
- (61) Gross, J.; Sadowski, G. Perturbed-Chain SAFT: An Equation of State Based on a Perturbation Theory for Chain Molecules. *Ind. Eng. Chem. Res.* **2001**, *40*, 1244–1260.
- (62) Gross, J.; Sadowski, G. Application of the Perturbed-Chain SAFT Equation of State to Associating Systems. *Ind. Eng. Chem. Res.* **2002**, *41*, 5510–5515.
- (63) Wertheim, M. S. Fluids with Highly Directional Attractive Forces: I. Statistical Thermodynamics. *J. Stat. Phys.* **1984**, *35*, 19–34.
- (64) Wertheim, M. S. Fluids with Highly Directional Attractive Forces: II. Thermodynamic Perturbation Theory and Integral Equations. *J. Stat. Phys.* **1984**, *35*, 35–47.
- (65) Wertheim, M. S. Fluids with Highly Directional Attractive Forces: III. Multiple Attraction Sites. *J. Stat. Phys.* **1986**, *42*, 459–476.
- (66) Wertheim, M. S. Fluids with Highly Directional Attractive Forces: IV. Equilibrium Polymerization. *J. Stat. Phys.* **1986**, *42*, 477–492.
- (67) Padaszyński, K.; Chiyen, J.; Ramjugernath, D.; Letcher, T. M.; Domańska, U. Liquid–Liquid Phase Equilibrium of Piperidinium-Based Ionic Liquid + an Alcohol Binary Systems and Modelling with NRHB and PCP-SAFT. *Fluid Phase Equilib.* **2011**, *305*, 43–52.
- (68) Huang, S. H.; Radosz, M. Equation of State for Small, Large, Polydisperse, and Associating Molecules. *Ind. Eng. Chem. Res.* **1990**, *29*, 2284–2294.
- (69) Wolbach, J. P.; Sandler, S. I. Using Molecular Orbital Calculations to Describe the Phase Behavior of Cross-Associating Mixtures. *Ind. Eng. Chem. Res.* **1998**, *37*, 2917–2928.
- (70) Held, C.; Neuhaus, T.; Sadowski, G. Compatible Solutes: Thermodynamic Properties and Biological Impact of Ectoines and Prolines. *Biophys. Chem.* **2010**, *152*, 28–39.
- (71) Orchillés, A. V.; Miguel, P. J.; González-Alfaro, V.; Vercher, E.; Martínez-Andreu, A. Isobaric Vapor–Liquid Equilibria of 1-Propanol + Water + Trifluoromethanesulfonate-Based Ionic Liquid Ternary Systems at 100 kPa. *J. Chem. Eng. Data* **2011**, *56*, 4454–4460.
- (72) Lungwitz, R.; Spange, S. A Hydrogen Bond Accepting (HBA) Scale for Anions, Including Room Temperature Ionic Liquids. *New J. Chem.* **2008**, *32*, 392–394.
- (73) Passos, H.; Ferreira, A. R.; Cláudio, A. F. M.; Coutinho, J. A. P.; Freire, M. G. Characterization of Aqueous Biphasic Systems Composed of Ionic Liquids and a Citrate-Based Biodegradable Salt. *Biochem. Eng. J.* **2012**, *67*, 68–76.
- (74) Rowley, R. L.; Wilding, W. V.; Oscarson, J. L.; Zundel, N. A.; Marshall, T. L.; Daubert, T. E.; Danner, R. P. *DIPPR Data Compilation of Pure Compound Properties*; Design Institute for Physical Properties; AIChE: New York, 2002.
- (75) Afeefy, H. Y.; Liebman, J. F.; Stein, S. E. Neutral Thermochemical Data In *NIST Chemistry WebBook*, NIST Standard Reference Database Number 69; Linstrom, P. J., Mallard, W. G., Eds.; National Institute of Standards and Technology, Gaithersburg, MD, June, 2005; p 20899 (<http://webbook.nist.gov>).
- (76) Held, C. *Measuring and Modeling Thermodynamic Properties of Biological Solutions*. Ph.D. Thesis, Technische Universität Dortmund, Dortmund, Germany, Dec., 2011.
- (77) Freire, M. G.; Carvalho, P. J.; Silva, A. M. S.; Santos, L. M. N. B. F.; Rebelo, L. P. N.; Marrucho, I. M.; Coutinho, J. A. P. Ion Specific Effects on the Mutual Solubilities of Water and Hydrophobic Ionic Liquids. *J. Phys. Chem. B* **2009**, *113*, 202–211.
- (78) Hofmeister, F. Zur Lehre von der Wirkung der Salze. *Arch. Exp. Pathol. Pharmacol.* **1888**, *24*, 247–260.
- (79) Mourão, T.; Cláudio, A. F. M.; Boal-Palheiros, I.; Freire, M. G.; Coutinho, J. A. P. Evaluation of the Impact of Phosphate Salts on the Formation of Ionic-Liquid-Based Aqueous Biphasic Systems. *J. Chem. Thermodyn.* **2012**, *54*, 398–405.
- (80) Robinson, R. A.; Stokes, R. H. *Electrolyte Solutions*, 2nd ed.; Courier Dover Publications: New York, 1970.
- (81) Lobo, V. M. M.; Quaresma, J. L. *Handbook of Electrolyte Solutions*; Elsevier: Amsterdam, 1989; Parts A and B.
- (82) Marcus, Y. *Ion Properties*; Marcel Dekker, Inc.: New York, 1997; Vol. 1, pp 124–125.
- (83) Yee, P.; Shah, J. K.; Maginn, E. J. State of Hydrophobic and Hydrophilic Ionic Liquids in Aqueous Solutions: Are the Ions Fully Dissociated? *J. Phys. Chem. B* **2013**, *117*, 12556–12566.
- (84) Held, C.; Cameretti, L. F.; Sadowski, G. Modeling Aqueous Electrolyte Solutions: Part 1. Fully Dissociated Electrolytes. *Fluid Phase Equilib.* **2008**, *270*, 87–96.
- (85) Robinson, R. A.; Harned, H. S. Some Aspects of the Thermodynamics of Strong Electrolytes from Electromotive Force and Vapor Pressure Measurements. *Chem. Rev.* **1941**, *28*, 419–476.
- (86) Köddermann, T.; Wertz, C.; Heintz, A.; Ludwig, R. Ion-Pair Formation in the Ionic Liquid 1-Ethyl-3-Methylimidazolium Bis-(triflyl)imide as a Function of Temperature and Concentration. *ChemPhysChem* **2006**, *7*, 1944–1949.
- (87) Almeida, H. F. D.; Passos, H.; Lopes-da-Silva, J. A.; Fernandes, A. M.; Freire, M. G.; Coutinho, J. A. P. Thermophysical Properties of Five Acetate-Based Ionic Liquids. *J. Chem. Eng. Data* **2012**, *57*, 3005–3013.
- (88) Domańska, U.; Królikowski, M. Phase Equilibria Study of the Binary Systems (1-Butyl-3-methylimidazolium Tosylate Ionic Liquid + Water, or Organic Solvent). *J. Chem. Thermodyn.* **2010**, *42*, 355–362.
- (89) Gardas, R. L.; Freire, M. G.; Carvalho, P. J.; Marrucho, I. M.; Fonseca, I. M. A.; Ferreira, A. G. M.; Coutinho, J. A. P. High-Pressure Densities and Derived Thermodynamic Properties of Imidazolium-Based Ionic Liquids. *J. Chem. Eng. Data* **2006**, *52*, 80–88.
- (90) Neves, C. M. S. S.; Kurnia, K. A.; Coutinho, J. A. P.; Marrucho, I. M.; Lopes, J. N. C.; Freire, M. G.; Rebelo, L. P. N. Systematic Study of the Thermophysical Properties of Imidazolium-Based Ionic Liquids with Cyano-functionalized Anions. *J. Phys. Chem. B* **2013**, *117*, 10271–10283.
- (91) Tshibangu, P. N.; Ndwandwe, S. N.; Dikio, E. D. Density, Viscosity, and Conductivity Study of 1-Butyl-3-methylimidazolium Bromide. *Int. J. Electrochem. Sci.* **2011**, *6*, 2201–2213.
- (92) Zech, O.; Stoppa, A.; Buchner, R.; Kunz, W. The Conductivity of Imidazolium-Based Ionic Liquids from (248 to 468) K. B. Variation of the Anion. *J. Chem. Eng. Data* **2010**, *55*, 1774–1778.
- (93) Khan, I.; Kurnia, K. A.; Saraiva, J. A.; Pinho, S. P.; Coutinho, J. A. P. Probing the Interactions between Ionic Liquids and Water: Experimental and Quantum Chemical Approach. *J. Phys. Chem. B* **2014**, DOI: 10.1021/jp4113552.

(94) Fuchs, D.; Fischer, J.; Tumakaka, F.; Sadowski, G. Solubility of Amino Acids: Influence of the pH Value and the Addition of Alcoholic Cosolvents on Aqueous Solubility. *Ind. Eng. Chem. Res.* **2006**, *45*, 6578–6584.